Dalton Transactions

Accepted Manuscript

ROYAL SOCIETY OF CHEMISTRY

www.rsc.org/dalton

pH-induced Dy_4 and Dy_{10} cluster-based 1D chains with different magnetic relaxation features

Zhi-Lei Wu,[a,b] Jie Dong,[b] Wei-Yan Ni, [b] Bo-Wen Zhang, [b] Jian-Zhong Cui[*a] and Bin Zhao[*b]

Abstract

Two novel tetra- and deca-nuclear dysprosium compounds, namely, $[Dy_4(\mu_3\text{-}OH)_2(L)_{10}(bipy)_2(H_2O)_2]_n$ (**1**) and $\{[Dy_{10}(\mu_3\text{-}OH)_8(L)_{22}(bipy)_2(H_2O)_2]\cdot 5H_2O\}_n$ (**2**) (L=3-Fluoro-4-(trifluoromethyl)benzoic acid; bipy=2,2'-bipyridine) have been successfully obtained by hydrothermal reaction at different pH. The solid state structures of **1** and **2** were established by single crystal X-ray diffraction technique, and both of them exhibit complicated 1D chains with $[Dy_4]$ (**1**) and $[Dy_{10}]$ (**2**) cluster units, respectively. Adjacent $[Dy_4]$ in **1** or $[Dy_{10}]$ in **2** are connected by two bridging carboxylate group in $\eta^1{:}\eta^1{:}\mu_2$ mode. Magnetic studies reveal that they exhibit different magnetic relaxation behaviors with the energy barrier of 23.6 K for **1** and 3.2 K for **2**. Interestingly, the large divergence in both structures and magnetic properties for **1** and **2** only originated from the different pH values in preparing them.

Introduction

Since the first single-molecule magnet (SMM), $[Mn]_{12}$ acetate, was discovered in the early 1990s, there have been great development in the field of molecular magnetism due to their huge potential applications in data storage and processing.[1] Various transition metal clusters were explored to pursuit the unique SMMs with both high ground spin state S and large negative zero-field-splitting parameter D. Nevertheless, it has been proved very difficult to simultaneously optimize both of them. Recently, the SMMs based on pure lanthanide ions arouse extensive interest in

[a] *Department of Chemistry, Tianjin University, Tianjin, 300072, China.*
E-mail: cuijianzhong@tju.edu.cn
[b] *Department of Chemistry, Key Laboratory of Advanced Energy Material Chemistry, MOE, TKL of Metal and Molecule Based Material Chemistry, and Collaborative Innovation Center of Chemical Science and Engineering (Tianjin), Nankai University, Tianjin 300071, China.*
E-mail: zhaobin@nankai.edu.cn
Electronic supplementary information (ESI) available: PXRD, coordination polyhedron of Dy(III) ions and other magnetic measurements. CCDC 989712 (**1**) and 989713 (**2**).

that some mononuclear compounds can show slow magnetic relaxation, which may be promising candidates for the design of SMMs with higher barrier due to their large intrinsic magnetic anisotropy. Amongst these studies, Dy(III) ions are widely employed to obtain SMMs due to the following features: 1) high-magnitude $\pm m_J$ quantum number and a doubly degenerate ground state due to its odd electron count; 2) the relatively large energy gap between its bistable electronic ground state. As a result, lots of Dy-based SMMs were reported with the different nuclearity like Dy_2,[2] Dy_3,[3] Dy_4,[4] Dy_5,[5] Dy_6,[6] Dy_7,[7] Dy_8,[8] Dy_9,[9] Dy_{10},[10] D_{11},[11] Dy_{12},[12] Dy_{14},[13] Dy_{24}[14] and Dy_{26},[15] of which some polynuclear clusters display complicated and interesting magnetic behaviors. Impressively, the square pyramidal $[Dy_5O(OiPr)_{13}]$ cluster shows the highest anisotropic barrier of 530 K and blocking temperature as high as 40 K.[16] The peculiar triangular Dy_3 cluster possesses unusual slow magnetic relaxations in spite of the almost non-magnetic ground state, and the intriguing behavior arises from the non-collinearity of the easy magnetization axis of three Dy(III) ions in the plane of the triangle. These results uncovered the different cluster structures resulted in the significant divergence of magnetic behavior. Therefore, in order to seek more polynuclear Dy-cluster SMMs with outstanding magnetic properties, it is necessary and crucial to explore how the synthetic conditions tuned the structures and magnetic properties of polynuclear Dy-cluster. Although the case that diversities of Dy-cluster structures depended on different anions has been observed,[17] pH-tuned the both structural and magnetic changes of polynuclear Dy-cluster has been hardly reported so far.

In this contribution, novel tetra- and deca-nuclearity Dy-cluster compounds $[Dy_4(\mu_3\text{-}OH)_2(L)_{10}(bipy)_2(H_2O)_2]_n$ (**1**) and $\{[Dy_{10}(\mu_3\text{-}OH)_8(L)_{22}(bipy)_2(H_2O)_2]\cdot 5H_2O\}_n$ (**2**) (L=3-Fluoro-4-(trifluoromethyl)benzoic acid; bipy=2,2'-bipyridine) were synthesized by only tuning pH value of the reactive system and without changing other conditions. They were structurally and magnetically characterized. The μ_3-OH bridges adjacent Dy^{3+} to form $[Dy_4(\mu_3\text{-}OH)_2]^{10+}$ ($[Dy_4]$, for short) in **1** and $[Dy_{10}(\mu_3\text{-}OH)_8]^{22+}$ ($[Dy_{10}]$, for short) cluster in **2**, respectively, and these clusters are further linked into 1D chains by carboxylic groups of the L^-. Magnetic investigations

reveal that both of them exhibit slow magnetic relaxation behaviors with the energy barrier of 23.6 K for **1** and 3.2 K for **2**. To the best of our knowledge, it is the first example that pH value play decisive roles in tuning structures and slow magnetic relaxation of polynuclear Dy-clusters.

Experimental Section

Materials and Methods

All chemicals were of commercial origin without further purification except that the $Dy(NO_3)_3 \cdot 6H_2O$ was prepared by HNO_3 and corresponding rare-earth oxide. The C, H, and N microanalyses were carried out at the Institute of Elemental Organic Chemistry, Nankai University. Powder X-ray Diffraction measurements were collected on a D/Max-2500 X-ray Diffractometer using Cu-K radiation. The magnetic measurements were carried out with a Quantum Design MPMS-XL7 and a PPMS-9 ACMS magnetometer.

Crystallographic studies

Single-crystal X-ray diffraction measurement of **1** was carried out on a Rigaku-RAPID diffractometer at 133(2) K equipped with graphite-monchromatic Mo*K*α radiation (λ = 0.71073 Å). Single-crystal X-ray diffraction measurement of **2** was carried out on a Bruker Smart Aepex CCD Single Crystal Diffractometer at 128(9)K equipped with graphite-monchromatic Mo*K*α radiation (λ = 0.71073 Å). The structures of **1** and **2** were solved by direct methods and refined by full-matrix least-squares techniques based on F^2 using the SHELXS-97 and SHELXS-2013 programs, respectively. All the non-hydrogen atoms were refined with anisotropic parameters while hydrogen atoms were placed in calculated positions and refined using a riding model. Because the guest water molecules severely disordered in compound **2**, the position of which cannot be determined by single crystal X-ray diffraction techniques, and therefore the SQUEEZE routine in the PLATON software package was applied. The elemental analyses of C, H, and N are close to that of calculated according to the molecular formula. The selected crystal parameters, data collection, and refinements are summarized in Table 1.

Table 1 Crystallographic Data for Compounds 1 and 2

Compound	1	2
Formula	$C_{100}H_{52}Dy_4F_{40}N_4O_{24}$	$C_{196}H_{104}Dy_{10}F_{88}N_4O_{59}$
Fw	3103.26	6755.69
Crystal system	*P*21/*c*	*P*21
Space group	monoclinic	monoclinic
a, Å	9.45	16.08
b, Å	31.33	32.03
c, Å	20.41	23.35
α, deg	90	90
ß, deg	117.58	107.38
γ , deg	90	90
V, $Å^3$	5358(2)	11475(4)
Z	4	2
Dc, mg/mm^3	1.924	1.929
μ, mm^{-1}	2.900	3.358
reflns collected	31924	78951
2θ range, deg	3.44-50.02	5.88-56
F(000)	2992	6364
GOF on F^2	1.094	1.024
R_1/ wR_2 (I>2σ(I))	R_1 = 0.0427, wR_2 = 0.1014	R_1 = 0.0507, wR_2 = 0.1216
R_1/ wR_2 (all data)	R_1 = 0.0454, wR_2 = 0.1043	R_1 = 0.0515, wR_2 = 0.1218

Synthesis

$[Dy_4(\mu_3\text{-}OH)_2(L)_{10}(bipy)_2(H_2O)_2]_n$ (1)

A mixture of L (0.3 mmol), $Dy(NO_3)_3$ (0.1 mmol) and bipy (0.1 mmol), 10mL distilled water were sealed in a Teflon-lined stainless vessel (25 mL) and heated at 160□ for 96 h, then the vessel was cooled slowly down to room temperature at 1.5□/h, affording the products as colorless needle shaped crystals. The yield was 72% based on Dy. Elemental analysis (%) calcd for: C, 41.89; H, 1.68; N, 1.80. Found: C, 41.71; H, 1.63; N, 1.72.

$\{[Dy_{10}(\mu_3\text{-}OH)_8(L)_{22}(bipy)_2(H_2O)_2]\cdot 5H_2O\}_n$ (2)

An aqueous solution of NaOH (0.3 M, 10 mL) was added dropwise to a mixture of L

(0.3 mmol), $Dy(NO_3)_3$ (0.1 mmol), bipy (0.1 mmol) and 10 mL distilled water until the pH reached about 10. The mixture was then sealed in a Teflon-lined stainless vessel (25 mL) and heated at 160□ for 96 h. The vessel was then cooled slowly down to room temperature at 1.5 □/h. Colorless needle shaped crystals were obtained at last. The yield was 34% based on Dy. Elemental analysis (%) calcd: C, 34.91; H, 1.54; N, 0.83. Found: C, 34.71; H, 1.39; N, 0.78.

Results and Discussion

Crystal structure of $[Dy_4(\mu_3\text{-}OH)_2(L)_{10}(bipy)_2(H_2O)_2]_n$ (1)

The solid state structure of **1** was revealed by single-crystal X-ray crystallography, and it exhibits complicated 1D chain with polynuclear [Dy_4] units. Compound **1** crystallizes in the monoclinic *P*21/*c* space group and consists of a nearly coplanar centrosymmetric [Dy_4] butterfly core, ten L, two 2,2'-bipyridine, and two water molecules (Fig. 1). The [Dy_4] core is composed of two scalene triangular [Dy_3] units, and the Dy1···Dy2, Dy1···Dy1A as well as Dy2···Dy1A distance is 4.253, 3.884, 3.986 Å, respectively. Two μ_3-O atoms locate on the opposite sides of the [Dy_4] plane with the deviation from the plane of about 0.45 Å. Dy1 and Dy2 are bridged by one carboxylic group, one μ_3-O atom, and one water molecule. Dy1A and Dy2 are bridged by one μ_3-O atom and two carboxylic groups with the Dy-O distances range from 2.299 to 2.542 Å, all of which are similar to previously reported Dy–O bond lengths.[5b] Both Dy1 and Dy2 have an eight coordination environment with O_8 set for Dy1 and O_6N_2 set for Dy2, displaying the distorted bicapped trigonal prism coordination geometry (Fig. S3, ESI). The Dy-N distances are 2.314 and 2.335 Å, respectively. In the tetra-nuclear Dy-clusters unit of compound **1**, two different binding modes can be observed for the ligand L^-. Two L^- anions bind Dy1 and Dy1A atoms in a η^1:μ_1-mode and eight L^- anions coordinate to Dy atoms in a η^1:η^1:μ_2-mode (Scheme 1). Finally, adjacent [Dy_4] cores are bridged into 1D chain by two carboxylate groups of L^- in η^1:η^1:μ_2 mode (Fig. S4, ESI), and the shortest Dy-Dy distance between adjacent clusters is 6.177 Å.

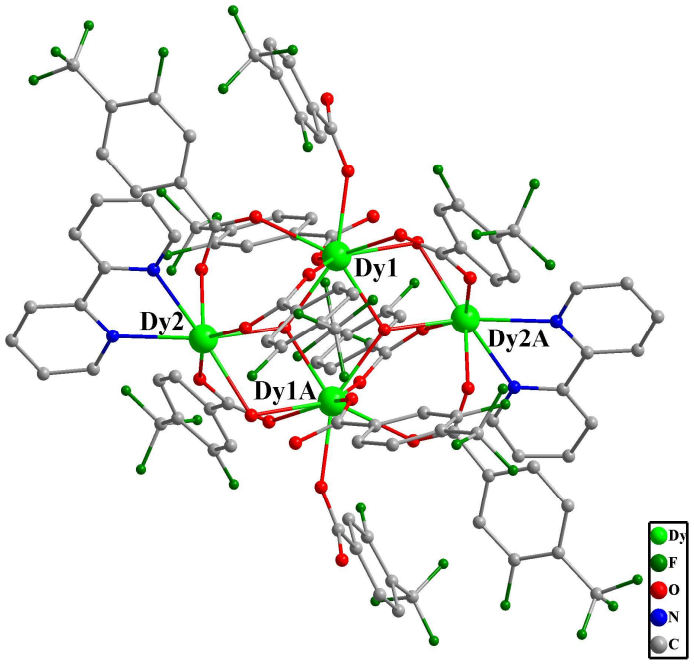

Fig. 1 Perspective view of the crystal structure of compound **1**, with all the hydrogen atoms omitted for clarity.

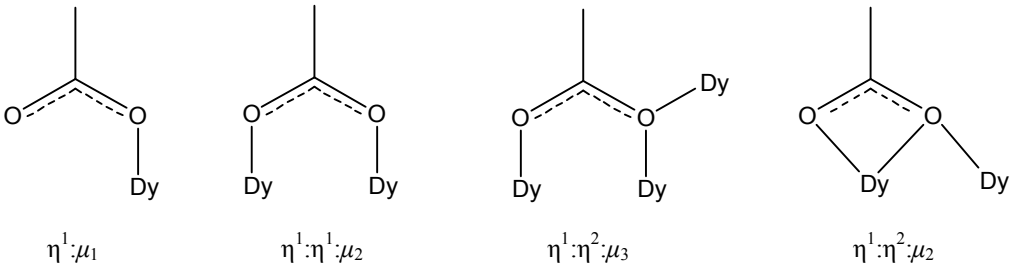

Scheme 1. Coordination modes of the ligand L^- observed in the compounds **1** and **2**.

Crystal structure of $\{[Dy_{10}(\mu_3\text{-}OH)_8(L)_{22}(bipy)_2(H_2O)_2]\cdot 5H_2O\}_n$ (2)

Structure analyses reveal that **2** also exhibits 1D chain with polynuclear [Dy_{10}] units, which crystallizes in the monoclinic *P*21 space group and consists of a [Dy_{10}] cluster, twenty-two L^- ligands, two 2,2'-bipyridine and two terminal water molecules (Fig. 2). Ten crystallographically independent Dy atoms exist in an asymmetric unit, and possess three types of coordination spheres: both Dy1 and Dy8 are coordinated by two N atoms from 2,2'-bipyridine and six O atoms from one μ_3-OH and four L; the coordination environments of Dy2, Dy3, Dy4, Dy5, Dy6, Dy7 and Dy9 are completed by eight O atoms from L^-, μ_3-OH and water molecules (three μ_3-OH and five carboxylate O for Dy2, Dy5, Dy7, and Dy9, four μ_3-OH and four carboxylate O for

Dy4 and Dy6, one μ_3-OH, one water molecules and six carboxylate O for Dy3); Dy10 atom is surrounded by nine O atoms from one μ_3-OH, one water molecules and five L^-. It should be noted that all Dy(III) ions from Dy1 to Dy9 are eight coordinated with bicapped trigonal prism geometries, while Dy10 is nine coordinated with a distorted mono-capped square anti-prism (Fig. S5, ESI). The lengths of Dy-O bonds fall into the range of 2.202 - 2.649 Å, and the range of Dy-N bond distances are 2.441 - 2.506 Å. For clarity, the [Dy_{10}] cluster core can be regarded as an assembly of eight edge-sharing Dy_3 triangle motifs (Fig. 3). Every three adjacent Dy(III) ions are linked by one μ_3-OH to give a trinuclear core of [$Dy_3(\mu_3$-OH)], which is further stabilized by the carboxylic groups of L^- ligands and 2,2'-bipyridine, resulting in a [Dy_{10}] core. In the deca-nuclear Dy-clusters unit of compound **2**, fifteen L^- anions coordinate in a η^1:η^1:μ_2-mode and two L^- anions employ η^1:η^2:μ_3-mode, while the other five L^- anions bind to Dy atoms in a η^1:η^2:μ_2-mode (Scheme 1). Similarly to **1**, adjacent [Dy_{10}] cores in **2** are further connected by two bridging carboxylate groups of ligands L^- in η^1:η^1:μ_2 mode into a 1D chain (Fig. 4c), and the shortest Dy-Dy separation between neighboring cores is 4.875 Å.

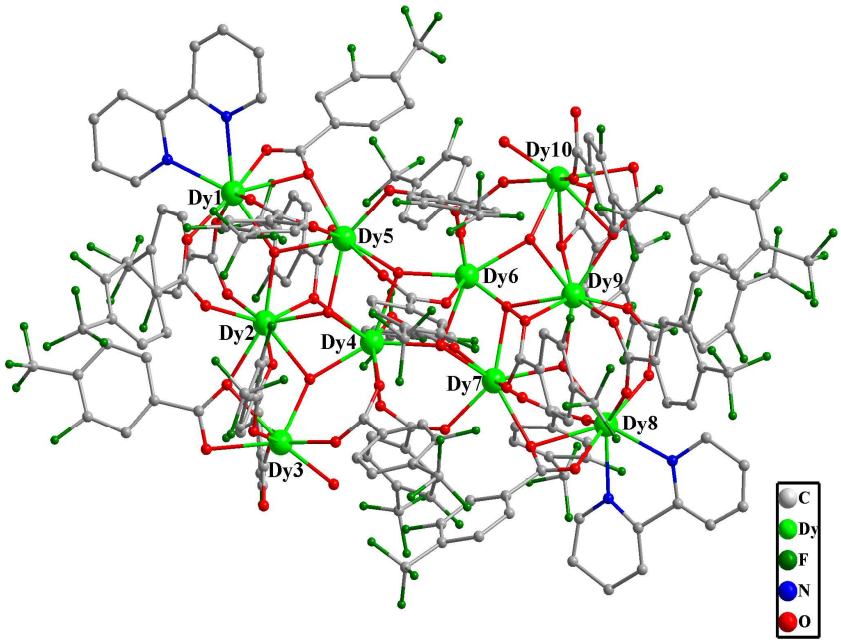

Fig. 2 Perspective view of the crystal structure of compound **2**, with all the hydrogen atoms omitted for clarity.

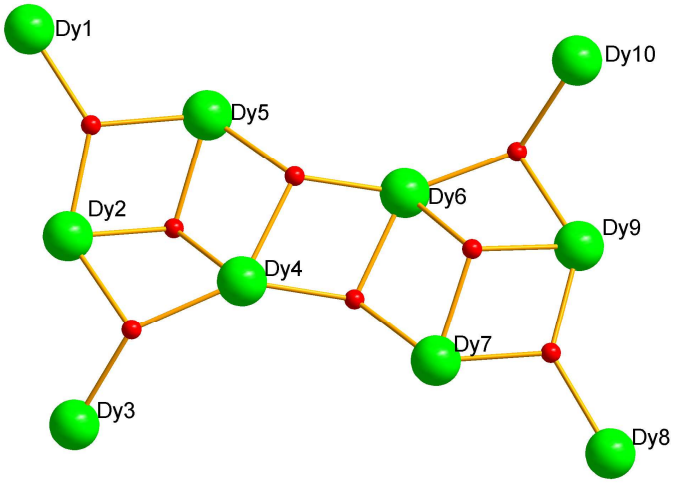

Fig. 3 Dy_3 triangles linked by the μ_3-OH in the $[Dy_{10}(\mu_3\text{-}OH)_8]^{22+}$ core.

Effect of the pH Value on the Structures

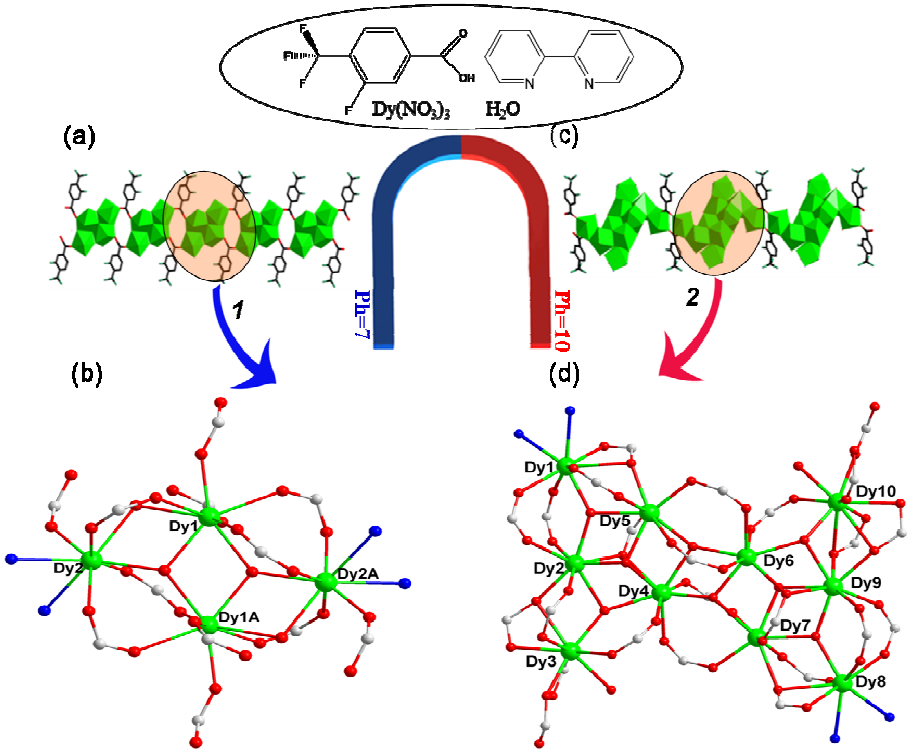

Fig. 4 The synthetic method of compounds **1** and **2**. (a) 1D chain structure in **1** consisted of $[Dy_4]$ clusters and carboxylate groups; (b) The structure of $[Dy_4]$ cluster; (c) 1D chain structure in **2** consisted of $[Dy_{10}]$ clusters and carboxylate groups; (d) The structure of $[Dy_{10}]$ cluster.

The relationship between the formations of **1** and **2** and the synthetic method of them are given in Fig 4. The results indicate that the pH value plays an important role in the formations of compounds **1** and **2**. By control of the pH value at 7, only

compound **1** can be obtained in which the 1D chain are consisted of [Dy_4] cluster. When the pH value of reaction system was adjusted to 10, compound **2** can be isolated as the only product, the structure of which is also a 1D chain, but consisted of [Dy_{10}] cluster. It should be noted that different coordination modes of the ligand L^- are observed in the compounds **1** and **2** (Scheme 1). In compound **1**, the ligands L^- employ η^1:μ_1- and η^1:η^1:μ_2-modes. However in **2**, three kinds of coordination modes of the ligand L^- were founded: η^1:η^1:μ_2-, η^1:η^2:μ_3-, and η^1:η^2:μ_2-modes. It indicates that different pH values can change the coordination pattern of ligand.

Up to now, many Dy_4 clusters have been reported with various structure types, including linear shape, square, butterfly, cube and so on. For example, Powell's group synthesized the first tetranuclear dysprosium compound with butterfly arrangement;[4c] Tang's group reported a linear- and square-shaped tetranuclear dysprosium compounds;[4f,4g] Liu's group gave a novel cube-like tetranuclear dysprosium.[4h] However, all reported tetranuclear dysprosium compounds are discrete clusters, and importantly, the butterfly-shaped [Dy_4] clusters in **1** are further assembled into 1D chain by carboxylate bridges, which is rather rare. Unlike Dy_4 clusters, decanuclear Dy-compounds have been little reported with only four examples, and their structure features are different from each other, including the ring-shaped Dy_{10} cluster synthesized by Westin's group,[10a] two trigonal prismatic Dy_5 units combined together by isonicotinate ligand in Murray's work,[10b] two [$Dy_5(\mu_3\text{-}OH)_2$] subcores connected through double acetate bridges into a Dy_{10} core in Tang's work,[10c] and recently, a new Dy_{10} cluster consisted of four edge-sharing [$Dy_4(\mu_4\text{-}O)$] tetrahedron, given by Tong's group.[10d] Comparably, the [Dy_{10}] cluster in **2** is unprecedented in reported decanuclear Dy-compounds, which is purely constructed by edge-sharing [$Dy_3(\mu_3\text{-}OH)$] triangles. Moreover, it is the first example of one-dimensional chain based on Dy_{10} cluster as node. The simulated and experimental powder X-ray diffraction patterns are well consistent from each other, indicative of that both **1** and **2** have good phase purity (Fig. S1 and S2, ESI).

Magnetic Properties

The direct-current (dc) magnetic susceptibility measurements of **1** and **2** have

been performed under a 1 kOe external field over temperature range 300-2 K. The plots of $\chi_M T$ *vs.* *T* (Fig. 5) indicate that two compounds show different behaviors. The observed $\chi_M T$ value of **1** and **2** at room temperature is 56.5 cm^3 K mol^{-1} and 143.8 cm^3 K mol^{-1}, respectively, which is in good agreement with the expected value for four uncoupled Dy(Ⅲ) ions (S=5/2, L=5, $^6H_{15/2}$, g=4/3 and C=14.17cm^3 K mol^{-1}) and ten uncoupled Dy(Ⅲ) ions. Upon decreasing the temperature, for **1**, the $\chi_M T$ value almost remains unchanged until 200K, then gradually decreases and reaches a minimum of 46.35 cm^3 K mol^{-1} at 10 K. For **2**, the $\chi_M T$ value declines quickly to 95.93 cm^3 K mol^{-1} at 10 K. Below 10 K, the $\chi_M T$ value increases rapidly to 49.64 cm^3 K mol^{-1} for **1** and declines sharply to 86.18 cm^3 K mol^{-1} for **2** at 2 K. The magnetic behavior of **1** indicates that the ferromagnetic interaction exists between Dy(Ⅲ) ions, which can compensate the decline of $\chi_M T$ caused by the thermal depopulation of the Dy(Ⅲ) excited states, so the $\chi_M T$ value almost keep unchanged from 300 to 200 K. However, for **2**, rapid decrease below 10 K may originate from the thermal depopulation of excited Stark sublevels and/or the weak antiferro-magnetic interactions between Dy(Ⅲ) ions. It should be noted the ferromagnetic interactions in **1** is rarely found in polynuclear lanthanide systems. The plots of *M vs. H/T* (Fig. S6, ESI) for **1** and **2** do not superimpose at different temperatures, and the unsaturated M value of 30.97 Nβ for **1** (45.1 Nβ for **2**) under the high field of 70 kOe and 2 K is far lower than the expected 40 Nβ (100 Nβ for **2**) (10 Nβ for each Dy(Ⅲ) ion with J = 15/2 and g = 4/3), indicating the presence of magnetic anisotropy and/or low-lying excited states.[18]

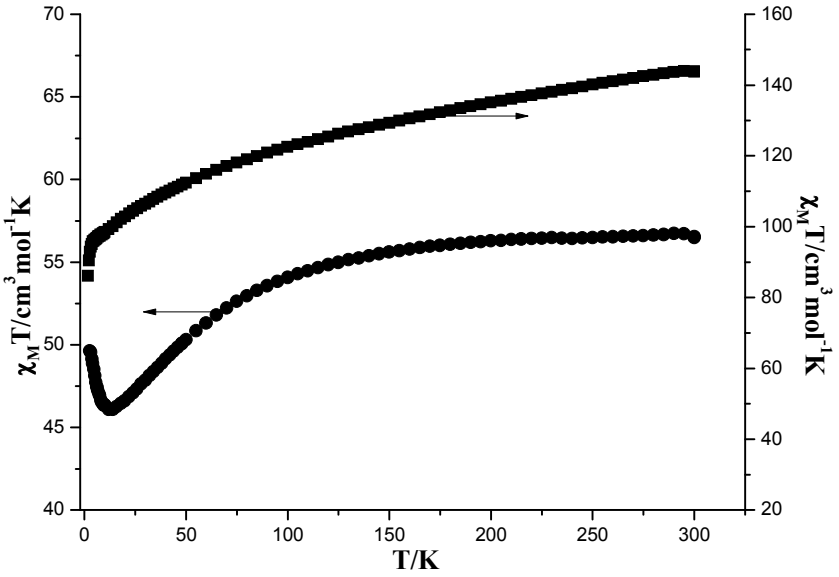

Fig. 5 Temperature dependence of the $\chi_M T$ products at 1000 Oe for compounds **1** (circle) and **2** (square).

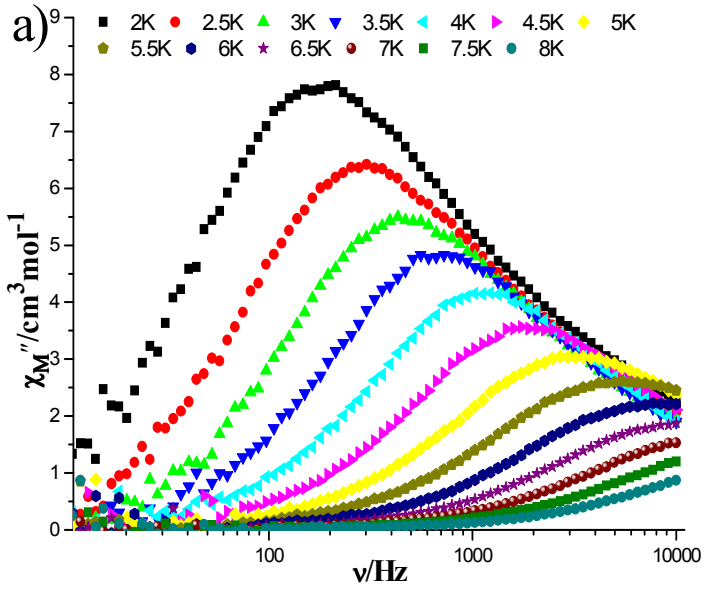

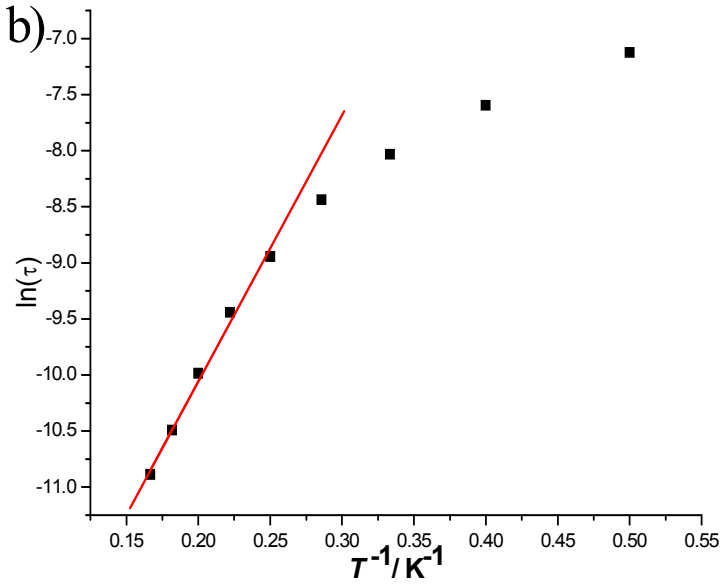

Fig. 6 (a) Frequency dependence of the out-of-phase ac susceptibility for compound **1**. (b) Magnetization relaxation time, ln(τ) *vs.* T^{-1} plot under H_{dc}= 0, the red line is fitted with the Arrhenius equation.

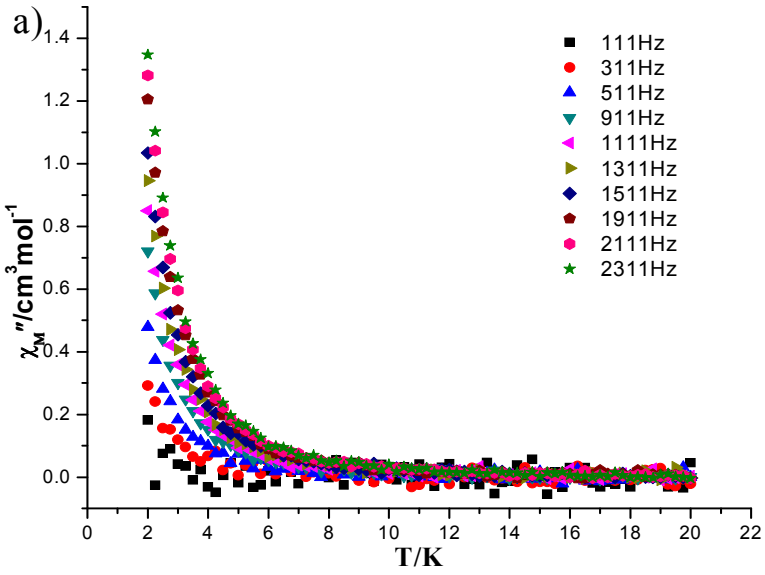

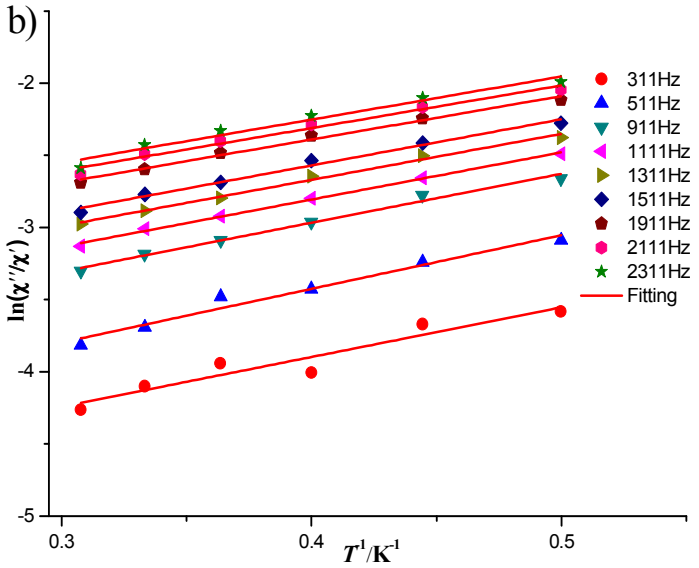

Fig. 7 (a) Temperature dependence of the out-of-phase signals of the ac susceptibility for **2** under a zero dc field (H_{ac}=3Oe). (b) Plots of natural logarithm χ''/χ' *vs.* $1/T$ for **2**. The solid red lines represent the fitting results over the range of 2.0- 3.25K.

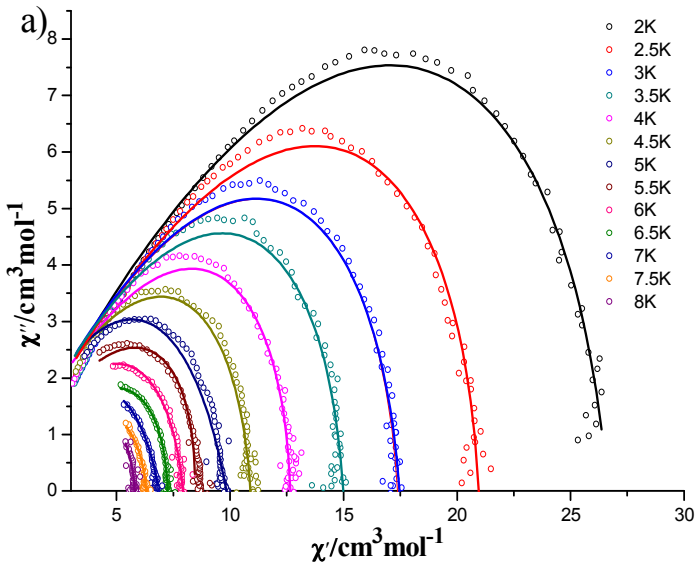

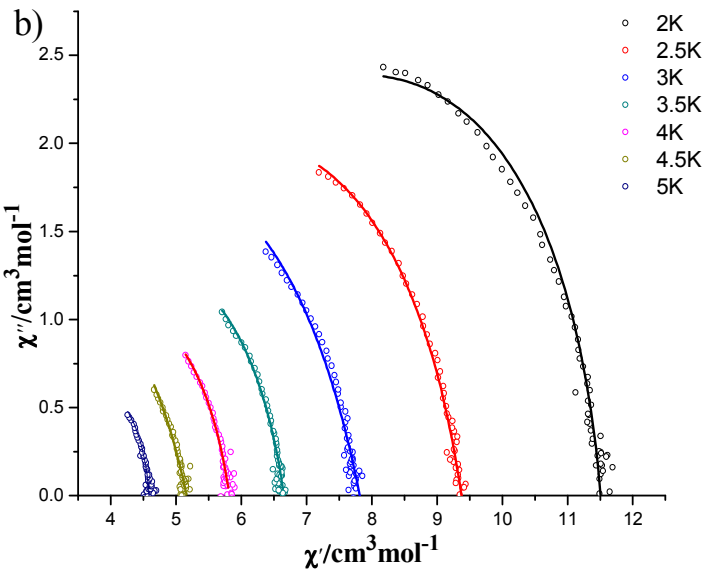

Fig. 8 Cole-Cole plots for **1** (a) and **2** (b). The solid lines are the best fits to the experimental data, obtained with the generalized Debye model.

In order to investigate the dynamics of the magnetization of **1** and **2**, the temperature and frequency dependencies of the alternating-current (ac) susceptibility were measured under the zero dc field (Fig. 6a, 7a and S7-S10 in ESI). Both of them show frequency-dependent out-of-phase (χ'') signals, suggesting a slow magnetic relaxation and SMM behavior. However, the peaks for only **1** are observed and not for **2**, which mainly related to the quantum tunneling effect commonly seen in lanthanide polynuclear compounds. The magnetic difference between **1** and **2** indicates that a stronger quantum tunneling in **2** occurs than that in **1**.[19] The Cole-Cole plots of χ'' *vs.* χ' for **1** and **2** were obtained and fitted to the generalized Debye model to obtain α values (Fig 8a and 8b).[20] For **1**, it shows nearly semi-circle shape and α= 0.22-0.40 was found over the temperature range of 2-8 K. However, the α=0.04-0.25 for compound **2** was obtained. Therefore, the relatively larger distribution coefficient α for **1** indicates compound **1** have a wider distribution of the relaxation time than that of **2**. The relaxation time of **1** was extracted from the frequency-dependent data between 2 and 6 K, and the relaxation energy barrier for **1** can be gotten by fitting τ values above 4 K and Arrhenius equation $\tau=\tau_0\exp(-\Delta E/k_BT)$, giving the pre-exponential factor $\tau_0 = 2.57*10^{-6}$ and the energy barrier $\Delta E/k_B$ = 23.6 K (Fig. 6b). In all reported [Dy_4] compounds (Table 2), the energy barriers vary from 3.3 to 173 K

in linear-shaped $[Dy_4(L)_4(CH_3OH)_6]$ given by Tang's group. But for the butterfly-shaped $[Dy_4]$ compounds, the energy barriers change from 3.7 to 170 K reported by Murugesu's group, and most of them is below 10 K. Comparably, the $\Delta E/k_B$ value of 23.6 K in **1** is relatively large. The parameter φ of 0.25 is obtained by the equation $\varphi = (\Delta T_p/T_p)/\Delta(\log f)$ and falls into the normal range ($0.1 < \varphi < 0.3$) expected for a superparamagnet, indicating that the magnetic behavior of compound **1** could not originate spin glass behavior. For all reported Dy_{10} clusters, they are similar to that of **2** with the absence of frequency-dependent peaks in out-of-phase susceptibility signals under zero dc field. Therefore, the relaxation barriers and pre-exponential factor τ_0 for **2** can not be obtained based on Arrhenius law. Provided that there is only one characteristic relaxation process in **2**, the energy barrier and the relaxation time can be roughly evaluated based on the Debye model and equation: $\ln(\chi''/\chi') = \ln(\omega\tau_0) + \Delta E/k_B T$,[18a,21] obtaining the energy barrier $\Delta E/k_B$ = 3.2 K and the relaxation time $\tau_0 = 1.32*10^{-6}$ (Fig. 7b). The τ_0 for both **1** and **2** agrees with expected value of 10^{-6}-10^{-12} s for a SMM.[22]

Table 2 Tetranuclear Dysprosium Compounds and their Energy Barriers

Structure types of Dy_4 clusters	The formula of Dy_4 compounds	Energy barrier /K	Pre-exponential factor
Linear-shape	$[Dy_4(L1)_4(CH_3OH)_6]$[4b]	173 19.7	1.2×10^{-7}, 7.8×10^{-6}
	$[Dy_4(L2)_4(HL2)_2(Anth)_2(CH_3OH)_4]$[4f]	20	---
	$[Dy_4(L3)_2(C_6H_5COO)_{12}(CH_3OH)_4]$[18b]	17.2	6.7×10^{-6}
Square-shape	$[Dy_4(L4)_4(OH)_4]Cl_2$[23]	---	---
	$[Dy_4(L4)_4(\mu_4\text{-}O)(\mu_2\text{-}1,1\text{-}N_3)_4]$[23]	91 51	4.5×10^{-7}, 3.0×10^{-9}
	$[Dy_4(HL5)_4(MeOH)_4]_2$[4g]	16 (900)	1.3×10^{-6}
	$[Dy_4(\mu_4\text{-}OH)(Hhpch)_8)]$[24]	30.3 16 6.2 3.3	3.0×10^{-5}, 3.7×10^{-5}, 1.96×10^{-3}, 1.82×10^{-4}
	$[Dy_4\{N(SiMe_3)_2\}_4(\mu\text{-}SEt)_8(\mu_4\text{-}SEt)]^{-}$[25]	66	4.3×10^{-6}
	$[Dy_4(\mu_3\text{-}OH)_2(bmh)_2(msh)_4Cl_2]$[26]	170 9.7	$4*10^{-7}$, $3.2*10^{-5}$
	$[Dy_4(H_3L6)_2(OAc)_6]$[27]	107 44	$2.0*10^{-7}$, $1.0*10^{-6}$
	$[Dy_4(\mu_3\text{-}OH)_2(\mu\text{-}OH)_2(2,2\text{-}bpt)_4(NO_3)_4(EtOH)_2]$[28]	80	$5.75*10^{-6}$

Butterfly-shape	Compound **1** in this work	23.57	$2.57*10^{-6}$
	$[Dy_4(\mu_3\text{-}OH)_2(hmmpH)_2(hmmp)(N_3)_4]$[4c]	7.0	$3.8*10^{-5}$
	$[Dy_4(\mu_3\text{-}OH)_2(mdeaH)_2(piv)_8]$[29]	6.2	$2.4*10^{-5}$
	$[Dy_4(\mu_3\text{-}OH)_2(ampdH_4)_2(piv)_{10}]$[30]	5.4	$1.1*10^{-5}$
	$[Dy_4(\mu_3\text{-}OH)_2(ovn)(piv)_4(NO_3)_2]$[31]	6.25	$3.75*10^{-5}$
	$[Dy_4(\mu_3\text{-}OH)_2(L7)_4(HL7)_2]$[32]	3.7	$4.8*10^{-5}$
	$[Dy_4(\mu_3\text{-}OH)_2(L8)_2(acac)_6]$[33]	22 (1400)	$3.66*10^{-6}$
	$[Dy_4(\mu_3\text{-}OH)_2(php)_2(OAc)_6(H_2O)_2]$[4a]	---	---
	$[Dy_4(\mu_3\text{-}OH)_2(hmmpH)_2(hmmp)_2(Cl)_4]$[4c]	---	---
Cube-shape	$[Dy_4(\mu_3\text{-}OH)_4(isonicotinate)_6(py)(CH_3OH)_7]](ClO_4)_2$[34]	40.2	1.1×10^{-11}
	$[Dy_4(OH)_4(TBSOC)_2(H_2O)_4(CH_3OH)_4]$ [4h]	22.9	1.1×10^{-8}
	$[Dy_4(HL9)_4(C_6H_4NH_2COO)_2(\mu_3\text{-}OH)_4(\mu\text{-}OH)_2(H_2O)]$[35]	---	---
	$[Dy_4(\mu_3\text{-}OH)_2(\mu_3\text{-}O)_2(cpt)_6(MeOH)_6(H_2O)]_2$[4d]	---	---

All the lattice solvents are omitted. The energy barrier are obtained without applying dc field, unless followed by a number in parentheses to indicate the strength of the applied dc field. The symbols "---" indicate that the values are not got in the references. The corresponding abbreviations of the ligands in the table are explained as following: HL1 = (2-hydroxy-3-methoxyphenyl)methylene hydrazide; HL2 = N-(2-carboxyphenyl)salicylidenimine; H(Anth) = anthranilic acid; HL3 = 2,6-bis((furan-2-ylmethylimino)methyl)-4-methylphenol; HL4 = ditopic carbohydrazone ligand; HL5 = *N*′, *N*″-(butane-2,3-diylidene)bis(2-hydroxy-3-methoxybenzohydrazide); Hhpch = 2-hydroxybenzaldehyde(pyridine-4-carbonyl); H_2bmh = bis(2-hydroxy-3-methoxybenzylidene); Hmsh = 3-methoxysalicylaldehyde hydrazone; H_3L6 = 1,3-bis[tris(hydroxymethyl)methylamino]propane; 2,2-Hbpt = 3,5-bis(2-pyridyl)-1,2,4-triazole; $hmmpH_2$ = 2-[(2-hydroxyethylimino)methyl]-6-methox-yphenol; H_2mdea = N-methyldiethanolamine; piv = pivalate; $ampdH_4$ = 3-amino-3-methylpentane-1,5-diol; Ovn = 3-methoxysalicylaldehydato anion; H_2L7 = (E)-2-(2-hydroxy-3-methoxybenzylideneamino)phenol; H_2L8 = *N*,*N*′-bis(salicylidene)-1,2-cyclohexanediamine); acac = acetylacetonate; H_2php = 2,6-(picolinoylhydrazone)pyridine); Py = pyridine; H_4TBSOC = p-tert-butylsulfonylcalix[4]arene; HL9 = 2-{[(2-hydroxy-3-methoxyphenyl)methylidene]amino}benzoic acid; Hcpt = 4-(4-carboxyphenyl)-1,2,4-triazole.

Conclusion

In summary, two novel $[Dy_4]$ and $[Dy_{10}]$ cluster-based 1D chains were structurally and magnetically characterized, and adjacent Dy(Ⅲ) ions in these clusters were bridged by μ_3-OH. Although various discrete $[Dy_4]$ and $[Dy_{10}]$ clusters have been well reported, the corresponding cluster-based 1D chains were hardly observed. Significant ferromagnetic interactions exhibit in **1** rather than **2**, and the different magnetic relaxation energy barriers were obtained. Interestingly, the large divergence in both structures and magnetic properties for **1** and **2** only originated from the different pH values in preparing them, and to our knowledge, it is rarely reported that pH value tunes the change of structures and slow magnetic relaxation in polynuclear

Dy-clusters. This work is wished to provide us inspiration in designing more novel polynuclear dysprosium clusters.

Acknowledgments

This work was supported by the 973 Program (2012CB821702 and 2011CB935902), NSFC (91122004 and 21473121), 111 project (B12015) and MOE Innovation Team (IRT13022 and IRT-13R30) of China.

Notes and references

1 A. Caneschi, D. Gatteschi, R. Sessoli, A. L. Barra, L. C. Brunel and M. Guillot, *J. Am. Chem. Soc.*, **1991**, 113, 5873.

2 (a) J. Long, F. Habib, P. H. Lin, I. Korobkov, G. Enright, L. Ungur, W. Wernsdorfer, L. F. Chibotaru and M. Murugesu, *J. Am. Chem. Soc.*, **2011**, 133, 5319; (b) F. Habib and M. Murugesu, *Chem. Soc. Rev.*, **2013**, 42, 3278.

3 (a) L. F. Chibotaru, L. Ungur and A. Soncini, *Angew. Chem., Int. Ed.*, **2008**, 47, 4126; (b) L. Ungur, W. V. d. Heuvel and L. F. Chibotaru, *New J. Chem.*, **2009**, 33, 1224.

4 (a) S. F. Xue, L. Zhao, Y. N. Guo, R. P. Deng, Y. Guo and J. K. Tang, *Dalton Trans.,* **2011,** 40, 8347; (b) Y. N. Guo, G. F. Xu, P. Gamez, L. Zhao, S. Y. Lin, R. P. Deng, J. K. Tang and H. J. Zhang, *J. Am. Chem. Soc.,* **2010**, 132, 8538; (c) Y. Z. Zheng, Y. H. Lan, C. E. Anson, A. K. Powell, *Inorg. Chem.,* **2008**, 47, 10813; (d) D. Savard, P. H. Lin, T. J. Burchell, I. Korobkov, W. Wernsdorfer, R. Clérac and M. Murugesu, *Inorg. Chem*., **2009**, 48, 11748; (e) Y. F. Bi, X. T. Wang, W. P. Liao, X. W. Wang, R. P. Deng, H. J. Zhang and S. Gao, *Inorg. Chem.,* **2009**, 48, 11743; (f) H. S. Ke, G. F. Xu, Y. N. Guo, P. Gamez, C. M. Beavers, S. J. Teat and J. K. Tang, *Chem. Commun.*, **2010**, 46, 6057; (g) S. F. Xue, L. Zhao, Y. N. Guo and J. K. Tang, *Dalton Trans.*, **2012**, 41, 351; (h) C. M. Liu, D. Q. Zhang, X. Hao, and D. B. Zhu, *Cryst. Growth Des.*, **2012**, 12, 2948.

5 (a) P. F. Shi, Y. Z. Zheng, X. Q. Zhao, G. Xiong, B. Zhao, F. F. Wan and P. Cheng, *Chem. Eur. J.*, **2012**, 18, 15086; (b) M. T. Gamer, Y. Lan, P. W. Roesky, A. K. Powell, R. Clerac, *Inorg. Chem.*, **2008**, 47, 6581.

6 (a) H. Q. Tian, M. Wang, L. Zhao, Y. N. Guo, Y. Guo, J. K. Tang and Z. L. Liu, *Chem. Eur. J.*, **2012**, 18, 442; (b) Y. L. Hou, G. Xiong, P. F. Shi, R. R. Cheng, J. Z. Cui and B. Zhao, *Chem. Commun*., **2013**, 49, 6066.

7 (a) J. W. Sharples, Y. Z. Zheng, F. Tuna, E. J. L. McInnes and D. Collison, *Chem. Commun*., **2011**, 47, 7650; (b) A. B. Canaj, D. I. Tzimopoulos, A. Philippidis, G. E. Kostakis and C. J. Milios, *Inorg. Chem.*, **2012**, 51, 7451.

8 (a) P. P. Yang, X. F. Gao, H. B. Song, S. Zhang, X. L. Mei, L. C. Li and D. Z. Liao, *Inorg. Chem.*, **2011**, 50, 720; (b) H. Q. Tian, L. Zhao. Y. N. Guo, J. K. Tang and Z. L. Liu, *Chem. Commun*., **2012**, 48, 708.

9 D. I. Alexandropoulos, S. Mukherjee, C. P. Papatriantafyllopoulou, C. P. Raptopoulou, V. Psycharis, V. Bekiari, G. Christou and T. C. Stamatatos, *Inorg. Chem.*, **2011**, 50, 11276.

10 (a) L. G. Westin, M. Kritikos and A. Caneschi, *Chem. Commun.*, **2003**, 1012; (b) S. K. Langley, B. Moubaraki and K. S. Murray, *Polyhedron.*, **2013**, 64, 255; (c) H. Ke, G. F. Xu, L. Zhao, J. K. Tang, X. Y. Zhang, H. J. Zhang, *Chem. Eur. J.*, **2009**, 15, 10335; (d) P. H. Guo, X. F. Liao, J. D. Leng and M. L. Tong, *Acta Chim. Sinica.*, **2013**, 71, 173.

11 (a) Y. L. Miao, J. L. Liu, J. Y. Li, J. D. Leng, Y. C. Ou and M. L. Tong, *Dalton Trans.*, **2011**, 40, 10229; (b) D. N. Woodruff, R. E. P. Winpenny and R. A. Layfield, *Chem. Rev.*, **2013**, 113, 5110.

12 Y. L. Miao, J. L. Liu, J. D. Leng, Z. J. Lin and M. L. Tong, *CrystEngComm.*, **2011**, 13, 3345.

13 X. L. Li, L. F. He, X. L. Feng, Y. Song, M. Hu, L. F. Han, X. J. Zheng, Z. H. Zhang and S. M. Fang, *CrystEngComm.*, **2011**, 13, 3643.

14 L. X. Chang, G. Xiong, L. Wang, P. Cheng and B. Zhao, *Chem. Commun*., **2013**, 49, 1055.

15 X. J. Gu, R. Clérac, A. Houri and D. F. Xue, *Inorg. Chim. Acta.*, **2008**, 361, 3873.

16 R. J. Blagg, C. A. Muryn, E. J. L. McInnes, F. Tuna and R. E. P. Winpenny, *Angew. Chem., Int. Ed.*, **2011**, 50, 6530.

17 (a) F. S. Guo, Y. C. Chen, L. L. Mao, W. Q. Lin, J. D. Leng, R. Tarasenko, M. Orendáč, J. Prokleška, V. Sechovský and M. L. Tong, *Chem. Eur. J.* **2013**, 19, 14876; (b) F. Yang, Q. Zhou, G. Zeng, G. H. Li, L. Gao, Z. Shi and S. H. Feng, *Dalton Trans.,* **2014**, 43, 1238.

18 G. Xiong, X. Y. Qin, P. F. Shi, Y. L. Hou, J. Z. Cui and B. Zhao, *Chem. Commun.*, **2014**, 50, 4255.

19 P. F. Shi, G. Xiong, B. Zhao, Z. Y. Zhang and P. Cheng, *Chem. Commun.*, **2013**, 49, 2338.

20 J. A. Mydosh, *Spin Glasses: An Experimental Introduction*, Taylor & Francis, London, **1993**.

21 S. Y. Lin, G. F. Xu, L. Zhao, Y. N. Guo, Y. Guo and J. K. Tang, *Dalton Trans.*, **2011**, 40, 8213.

22 G. Xiong, H, Xu, J. Z. Cui, Q. L. Wang and B. Zhao, *Dalton Trans.*, **2014**, 43, 5639.

23 M. U. Anwar, L. K. Thompson, L. N. Dawe, F. Habib and M. Murugesu, *Chem. Commun.*, **2012**, 48, 4576.

24 S. F. Xue, L. Zhao, Y. N. Guo, X. H. Chen and J. K. Tang, *Chem. Commun.*, **2012**, 48, 7031.

25 D. N. Woodruff, F. Tuna, M. Bodensteiner, R. E. P. Winpenny and R. A. Layfield, *Organometallics.*, **2013**, 32, 1224.

26 P. H. Lin, T. J. Burchell, L. Ungur, L. F. Chibotaru, W. Wernsdorfer and M. Murugesu, *Angew. Chem., Int. Ed.*, **2009**, 48, 9489.

27 C. M. Liu, D. Q. Zhang and D. B. Zhu, *Dalton Trans.*, **2013**, 42, 14813.

28 P. H. Guo, J. L. Liu, Z. M. Zhang, L. Ungur, L. F. Chibotaru, J. D. Leng, F. S. Guo and M. L. Tong, *Inorg. Chem.*, **2012**, 51, 1233.

29 G. Abbas, Y. H. Lan, G. E. Kostakis, W. Wernsdorfer, C. E. Anson and A. K. Powell, *Inorg. Chem.*, **2010**, 49, 8067.

30 G. Abbas, G. E. Kostakis, Y. H. Lan and A. K. Powell, *Polyhedron.*, **2012**, 41, 1.

31 S. K. Langley, N. F. Chilton, I. A. Gass, B. Moubaraki and K. S. Murray, *Dalton Trans.*, **2011**, 40, 12656.

32 K. C. Mondal, G. E. Kostakis, Y. H. Lan, A. K. Powell, *Polyhedron.*, **2013**, 66, 268.

33 P. F. Yan, P. H. Lin, F. Habib, T. Aharen, M. Murugesu, Z. P. Deng, G. M. Li and W. B. Sun, *Inorg. Chem.*, **2011**, 50, 7059.

34 Y. J. Gao, G. F. Xu, L. Zhao, J. K. Tang and Z. L. Liu, *Inorg. Chem.*, **2009**, 48, 11495.

35 H. S. Ke, P. Gamez, L. Zhao, G. F. Xu, S. F. Xue and J. K. Tang, *Inorg. Chem.*, **2010**, 49, 7549.

Table of contents

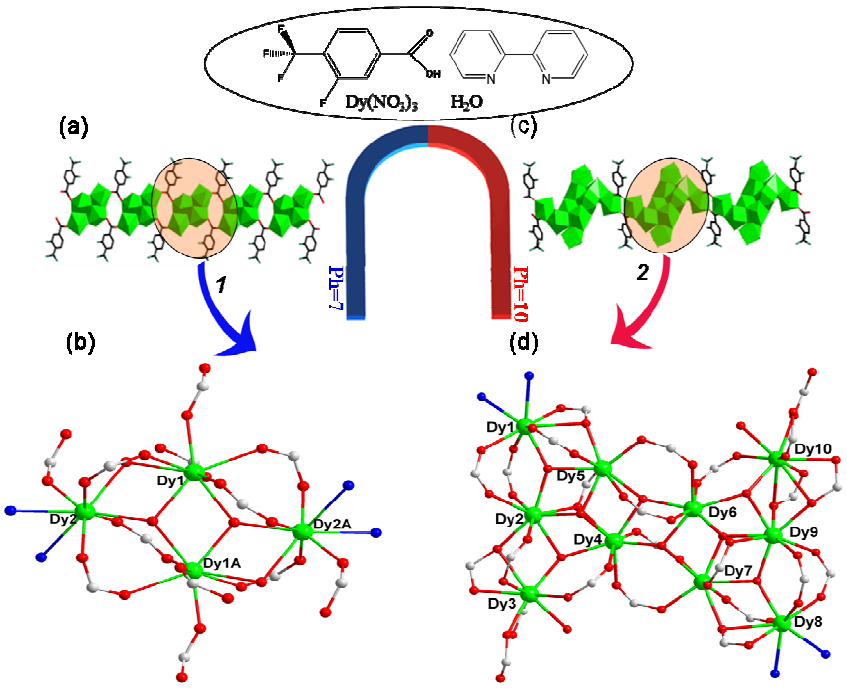

Two novel [Dy_4] and [Dy_{10}] cluster-based 1D chains (**1** and **2**) were structurally and magnetically characterized, exhibiting different magnetic relaxation behaviors. The results revealed that the different pH values induced the large structural and magnetic changes of **1** and **2**, and this is rarely reported in polynuclear Dy-clusters.